Rare Metal Materials and Engineering
Volume 49, Issue 9, September 2020
Available online at www.rmme.ac.cn

Science Press

Cite this article as: Rare Metal Materials and Engineering, 2020, 49(9): 2983-2990.

ARTICLE

Microstructure Characteristics and Thermodynamic Calculation of Nickel-based Corrosion Resistant Hastelloy G3 Alloy

Zhao Zhenduo[1], Li Sha[1], Fan Guangwei[1], Li Jianchun[2]

[1] *State Key Laboratory of Advanced Stainless Steel Materials, Taiyuan Iron and Steel（Group）Co., Ltd, Taiyuan 030003, China;*
[2] *Technology Center, Shanxi Taigang Stainless Steel Co., Ltd, Taiyuan 030003, China*

Abstract: Thermo-Calc software was used to calculate the thermodynamics of nickel-based corrosion resistant Hastelloy G3 alloy, and the influence of composition on the precipitation of equilibrium phase was studied. The precipitated phase of the alloy after aging treatment was observed by SEM and TEM. The results show that the equilibrium phases of alloy precipitation are mainly σ phase, μ phase, M_6C and $M_{23}C_6$ carbides; the content of Cr and Mo mainly affect the precipitation of σ phase and μ phase and the initial precipitation temperature; while the content of C significantly affects the precipitation behavior of carbides M_6C and $M_{23}C_6$. The precipitation rule of precipitates during the aging process was further studied through experiments.

Key words: Hastelloy G3 alloy; thermodynamic calculation; precipitated phase; aging treatment

Nickel-based corrosion resistant alloys have the ability to resist various forms of corrosion damage, such as pitting corrosion, crevice corrosion, stress corrosion and high chloride ion corrosion. Their comprehensive corrosion resistance is far superior to that of the stainless steel, especially suitable for the harsh and complex industrial fields that the stainless steel can not compete with [1-10]. Hastelloy G3 alloy is a typical nickel-based corrosion resistant alloy with ultra-low carbon, high Ni, Cr and Mo, containing a certain amount of alloying elements such as Cu, Co and W; it has excellent corrosion resistance [11-17]. It has an outstanding corrosion resistance in oxidizing and reducing media, and has been widely used in chemical industry, alkali making, paper making, sulfuric acid and phosphoric acid production and processing industries. The alloy has also attracted widespread attention as oil well tube material for high temperature and high acidity oil and gas fields [18-28]. In the actual production process of G3 alloy seamless tubes, the precipitation amount, precipitation and resolving temperature of precipitated phases in different batches of alloys will change due to the difference of the content of main alloying elements, while in the process of hot processing (including forging and extruding) and heat treatment (including intermediate annealing and solid solution treatment), if the process parameters are not selected properly, precipitates will appear in the grain boundaries and grains[29]. The precipitated phases in the corrosion resistant G3 alloys are mainly $M_{23}C_6$, M_6C, intermetallic compounds phase σ and μ; they are generally considered to be harmful phases, which will seriously affect the corrosion resistance and mechanical properties of the alloy. In view of this, the Thermo-Calc thermodynamic calculation software and the corresponding nickel-based alloy database were be used in this paper. The effects of precipitated phases and chemical composition on the precipitation rule of carbide phase and intermetallic compound phase in the alloy were studied, and the precipitation behavior of each phase in the corrosion-resistant G3 alloy was revealed. The precipitates of the alloy under different aging conditions were analyzed by metallographic microscope, SEM and TEM, which provided important

Received date: September 25, 2019
Foundation item: The Youth Top Talents Support Project of Shanxi Province (201606); The Natural Science Foundation of Shanxi Province (201801D121081)
Corresponding author: Zhao Zhenduo, Ph. D., Professorate Senior Engineer, State Key Laboratory of Advanced Stainless Steel Materials, Taiyuan Iron and Steel (Group) Co., Ltd, Taiyuan 030003, P. R. China, Tel: 0086-351-2130309, E-mail: zhaozd@tisco.com.cn

theoretical basis and experimental basis for the composition design, production process selection, precipitate control and reasonable formulation of heat treatment of the alloy.

1 Experiment

Thermo-Calc thermodynamic calculation software with TCSAB nickel-based alloy database was used to calculate the thermodynamic properties of G3 alloy. The alloy system was 1 mol, while the reference state was 298.15 K and 105 Pa. The components of the alloy system were input according to the mass fraction. By calculating the thermal equilibrium phase diagram, the possible precipitated equilibrium phases were obtained, the influence of chemical composition on precipitated phases was predicted, and the precipitation rules of each phase were revealed. The samples were taken from tube blanks through the VIM+ESR+forging, and 20 mm×20 mm×20 mm sample specimens were cut for the solid solution and aging treatment. The solid solution system was 1200 °C and 1 h, water-cooling; the aging system was 700~830 °C, aging for 2 h, 48 h, water-cooling. After the mechanical grinding and polishing, the aged specimens were etched by the solution of 1.5 g $CuSO_4$+40 mL HCl+20 mL anhydrous ethanol, and the microstructure was observed by SEM. Transmission electron microscopy (TEM) metal film samples were prepared by the double-spray electrolysis. The electrolyte was 5% potassium chlorate and ethanol mixture. The electrolyte was cooled by the liquid nitrogen. The working voltage was 40 V and the current was 40 mA. The temperature was controlled at 40 °C below zero. The morphology of the precipitated phase at grain boundary and in grain was observed by TEM and analyzed by the selected area electron diffraction.

2 Results and Discussion

2.1 Thermodynamic equilibrium phase diagram

Typical chemical composition of G3 alloy (wt%) is 0.012 C, 22.67 Cr, 1.94 Cu, 7.06 Mo, 0.85 W, 20.05 Fe and balance Ni. The thermodynamic equilibrium phase calculation shows that the relationship between the precipitation amount of each phase and temperature is shown in Fig.1. It can be seen from Fig.1 that the main equilibrium precipitates of the alloy are σ phase, μ phase, M_6C and $M_{23}C_6$ carbide. The initial melting point and final melting point of the alloy are 1353 and 1395 °C respectively, and the solidification range is only 42 °C. The initial precipitation temperature of the σ phase is 935 °C, and the precipitation amount peaks at 598 °C, and the maximum precipitation amount is 16.82%. The precipitated carbide at the high temperature is M_6C. The precipitation temperature ranges from 1067 °C to 834 °C, and the maximum precipitation amount is 0.432%. The initial precipitation temperature of the μ phase is 597 °C, and the precipitation amount increases with the decrease of temperature.

It is reported in Ref. [5] that the alloy will precipitate a μ phase after long-term aging. When the atomic percentage of W and Mo content in the nickel-based alloy is more than 3.5, the μ phase will be formed. After the formation of the μ phase, the local depletion of Mo will be caused, and the corrosion resistance will be reduced. Because the thermodynamic calculation results are stable equilibrium phases, the μ phase may gradually precipitate during the long-term use of the alloy.

2.2 Effect of alloy composition on melting point

The initial melting point of alloy is a very important parameter, and its change will directly affect the homogenization treatment and hot working temperature. Therefore, the effect of element content on the initial melting point should be considered in the composition design. Table 1 shows the change of the initial melting point and final melting point with the content of Cr and Mo, indicating both of them decrease with the increase of the content of Cr and Mo. In addition, if the elements of Cr and Mo are simultaneously increased to 23.5% and 8%, the initial melting point will decrease to 1337 °C, which has a great influence on the actual production of the alloy. Cr and Mo are the main alloy elements of Hastelloy G3. They can improve the corrosion resistance of the alloy by enhancing the density of passivation film. Increasing the content of Cr and Mo are beneficial to

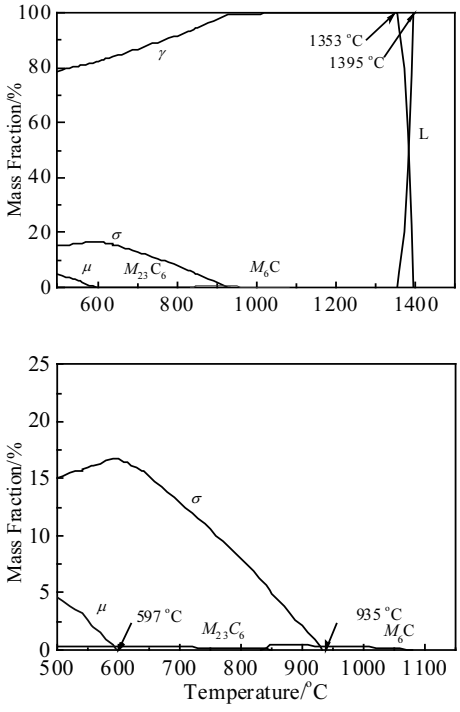

Fig.1 Equilibrium phase diagram and its partial enlarged view of precipitation amount of each phase in G3 alloy

the corrosion resistance of the alloy. Considering the production cost of the alloy and the influence of the decrease of the initial melting point of the alloy, thus increasing the difficulty of hot working, however, the content of Cr and Mo is not suitable to take the upper limit.

2.3 Equilibrium phase precipitation rules

2.3.1 Effect of alloy compositions on M_6C

The main element of carbide M_6C is Mo, which contains a certain amount of Cr. Fig.2 shows the effect of the content of Cr, Mo and C on the precipitation amount and the initial precipitation temperature of M_6C. It can be seen from it that the effect of Cr on the precipitation phase content of M_6C is not significant, basically maintained in the range of 0.36 wt%~0.47 wt%, and the precipitation temperature drops from 1071 °C to 1060 °C. Mo element has a slight influence on the content of the precipitated phase of M_6C. When the content of Mo increases from 6.0 wt% to 8.0 wt%, the amount of precipitated phase of M_6C increases from 0.34 wt% to 0.44 wt%, and the precipitation temperature rises from 1040 °C to 1086 °C. The C element has a significant effect on the precipitation and precipitation temperature of M_6C. The precipitation amount of M_6C increases linearly from 0.39 wt% at 0.01 wt% C to 1.16 wt% at 0.03 wt% C. The precipitation temperature also increases greatly with the increase of C content. The precipitation temperature rises from 1036 °C at 0.01 wt% C to 1152 °C at 0.03 wt% C.

2.3.2 Effect of alloy composition on carbide $M_{23}C_6$

The alloying elements of carbide $M_{23}C_6$ are mainly Cr and Mo, which are often distributed in the grain boundaries in a chain form. Fig.3 shows the relationship of the content of Cr, Mo and C with the precipitation amount and initial precipitation temperature of $M_{23}C_6$. It can be seen that the change of the content of Cr and Mo has little effect on the precipitation amount of $M_{23}C_6$, which is maintained at about 0.235 wt%, but has a significant effect on the precipitation temperature of $M_{23}C_6$. When the content of Cr increases from 21 wt% to 23.5 wt%, the precipitation temperature of $M_{23}C_6$ rises from 752 °C to 917 °C. The precipitation temperature of $M_{23}C_6$ decreases obviously with the increase of Mo content. When Mo content increases from 6.0 wt% to 8.0 wt%, the precipitation temperature of $M_{23}C_6$ decreases from 930 °C to 825 °C. When C content is 0.01 wt%, 0.02 wt% and 0.03 wt%, the precipitation amount of $M_{23}C_6$ reach 0.20 wt%, 0.39 wt% and 0.58 wt%, respectively, and the precipitation temperatures are 751, 759 and 766 °C, respectively.

Table 1 Effect of alloy composition Cr and Mo on the melting point

Element	Content/ wt%	Initial melting point/°C	Final melting point/°C
Cr	21.0	1371	1402
	22.5	1362	1395
	23.5	1360	1395
Mo	6.0	1370	1402
	7.0	1362	1395
	8.0	1357	1393

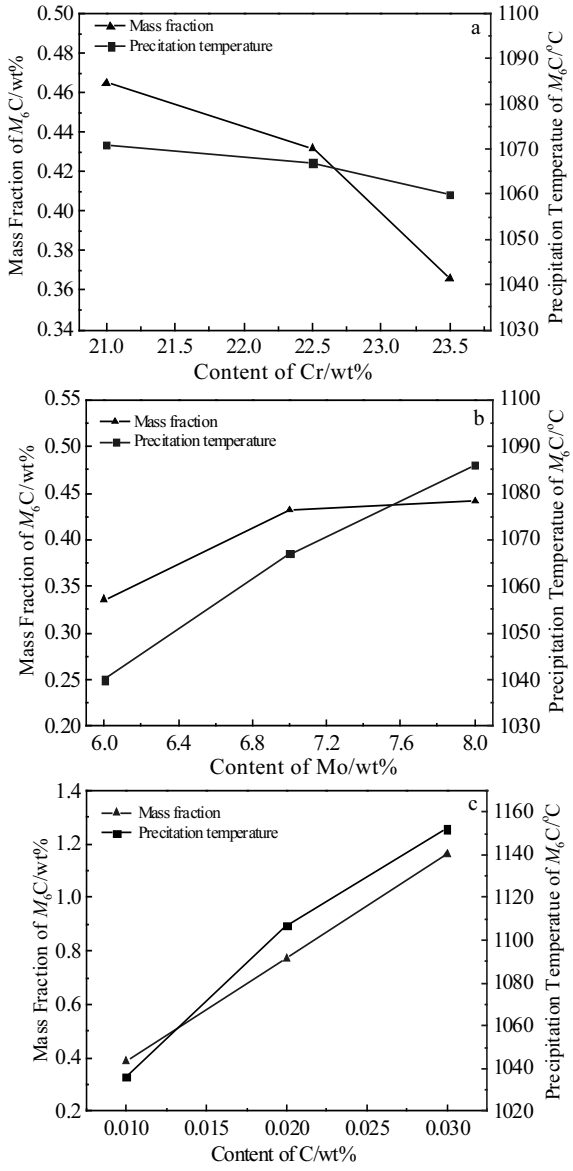

Fig.2 Effect of Cr (a), Mo (b) and C (c) contents on the precipitation amount and temperature of M_6C

The above results show that Cr and Mo have little effect on the precipitation amount of $M_{23}C_6$. The precipitation temperature of $M_{23}C_6$ increases with the increase of Cr content, while the effect of Mo is just opposite. The precipitation amount and temperature of $M_{23}C_6$ increase with the increase of C content, indicating that the decisive element affecting the precipitation amount of $M_{23}C_6$ is C. Therefore, the low content C should be controlled in com-

position design to avoid the precipitation of excessive carbide $M_{23}C_6$ to reduce the corrosion resistance of the alloy.

2.3.3 Effect of alloy composition on the precipitation of σ phase

The σ phase is an intermetallic compound rich in Cr and Mo. Therefore, the effect of Cr and Mo on its precipitation behavior is mainly calculated. Fig.4 shows the effect of Cr and Mo content on the maximum precipitation amount and initial precipitation temperature of the σ phase. In general, both Cr and Mo have great influence on the precipitation behavior of the σ phase. When the content of Cr increases, the precipitation amount and precipitation temperature of the phase increase to a great extent. When the content of Cr is 21.0 wt%, 22.5 wt% and 23.5 wt%, the precipitation temperature of the σ phase is 879, 933 and 962 °C, respectively. The precipitation peaks are 8.44%, 16.8% and 19.99%. At the same time, the precipitation temperature corresponding to the peak value of the σ phase also has some influence. The temperatures corresponding to the peak values show a downward trend, which are 730, 599 and 540 °C, respectively. With the increase of Mo content, the precipitation amount and temperature of σ phase also increase obviously. With the increase of Mo content, precipitation temperatures of σ phase are 871, 933 and 985 °C, respectively. The precipitation peaks are 14.43%, 16.78% and 16.98%, respectively. However, the temperature corresponding to precipitation peak of the σ phase is opposite to the influence of Cr element, and the temperature corresponding to the precipitation peak increases, which is 567, 595 and 663 °C, respectively. The σ phase is a harmful phase to the corrosion resistant alloy. The effect of Cr and Mo on σ phase should be considered in the alloy design. During the heat treatment, more Cr and Mo should be dissolved in matrix γ phase as much as possible to reduce the σ equivalent phase out.

2.3.4 Effect of alloy composition on the precipitation of μ phase

The studies have shown that, the μ phase is transformed from σ phase in the long-term aging process of the alloy,

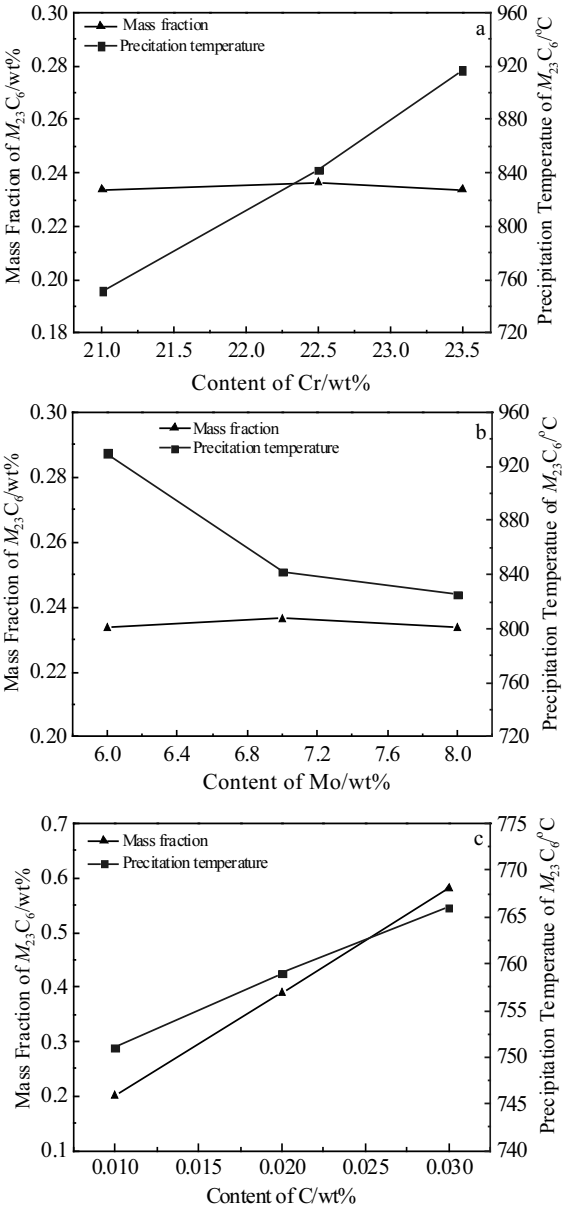

Fig.3 Effects of Cr (a), Mo (b) and C (c) contents on precipitation amount and temperature of $M_{23}C_6$

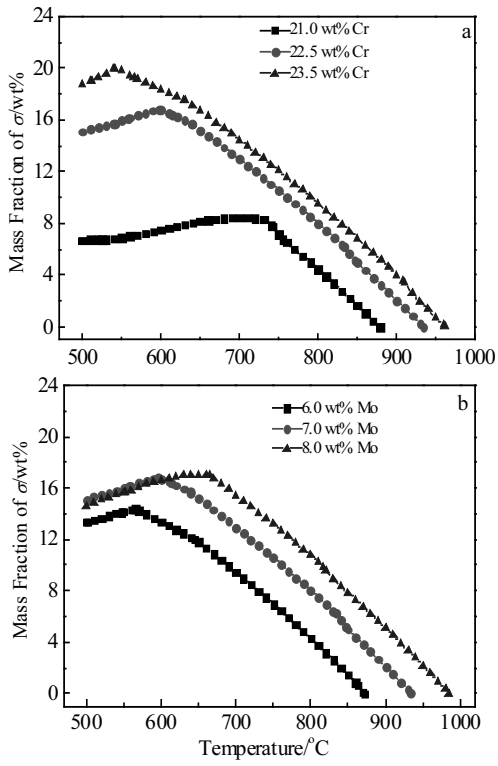

Fig.4 Relationship of precipitation amount and precipitation temperature of σ phase with different Cr (a) and Mo (b) contents

which is a harmful phase in the corrosion resistant alloy, and which will result in partial deficiency of Cr and Mo [30]. The μ phase belongs to the trigonal system, and there are 13 atoms in the unit cell. Compared with the σ phase, the μ phase is larger in size and has no strengthening effect. The shape of μ phase is generally granular, rod-like and block-like. Fig.5 shows the effect of the content of Cr and Mo on the precipitation of μ phase. It can be seen from Fig.5 that increasing the Cr content can significantly reduce the precipitation amount of the μ phase. When the Cr content is 21.0 wt%, the precipitation amount of the μ phase is 9.31%, and when the Cr content is 23.5%, the precipitation amount of the μ phase is 2.69%, and Cr causes a significant decrease in the precipitation temperature of the μ phase. As the Mo content increases from 6.0% to 8.0%, the initial precipitation temperature of the μ phase increases from 566 °C to 665 °C, and the precipitation amount of the μ phase increases from 3.41% to 7.05%. It can be seen that the Cr element inhibits the precipitation of the μ phase, and the Mo element promotes the precipitation of the μ phase. Therefore, in order to avoid the precipitation of the μ phase in the process of use, the content of Cr and Mo should be reasonably matched.

2.4 Effect of aging treatment on the precipitation of precipitated phase

The precipitation behavior of the precipitated phase was studied by the aging treatment of solid solution G3 alloy. The morphology of the precipitated phase after ageing at 700~830 °C for 2 h is shown in Fig.6. It can be seen from Fig.6 that after the aging treatment at different temperatures, the precipitated phase is found in the grain boundary, and no precipitated phase is found in the grain. This is due to the large number of dislocations in the grain boundaries, which easily provides energy for the nucleation of precipitated phases and makes precipitated phases precipitate preferentially in the grain boundaries.

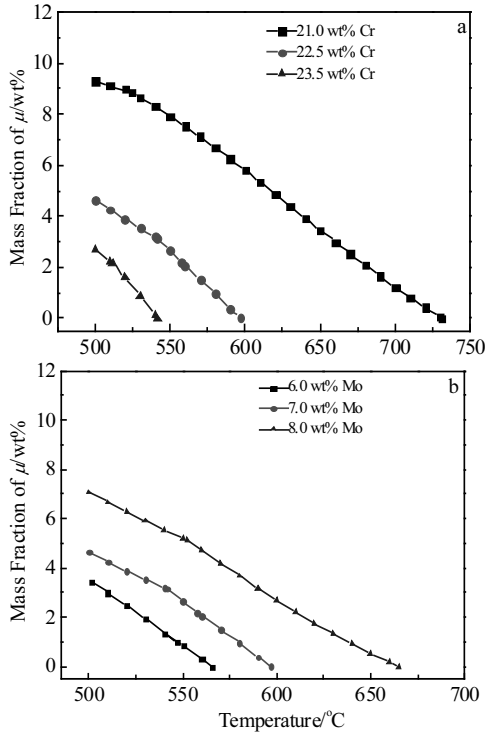

Fig.5 Relationship of precipitation amount and precipitation temperature of μ phase with different Cr (a) and Mo (b) contents

According to the EDS spectrum analysis of the grain boundary precipitates under the different aging temperatures, compared with the alloy matrix composition, the Cr content is greatly increased, the Mo content is slightly decreased, and the Fe and Ni contents are also decreased. Combined with thermodynamic calculation results and the results reported in Ref. [31], the precipitates are $M_{23}C_6$ carbide. It can also be seen that the number and size of precipitated phases at grain boundaries increase with the aging temperature rising in the range of 700~770 °C. The analysis shows that the increase of the aging temperature accelerates the diffusion of alloy elements, the phase change driving force increases, which resulting in the increase of nucleation and growth rate of $M_{23}C_6$. It is noteworthy that some precipitates at grain boundaries are discontinuous and almost perpendicular to the grain boundaries after aging at 770 °C, and the grain boundaries are widened to 3~7 μm. According to the analysis in Ref. [32], the phenomenon is controlled by the nucleation and growth mechanism of $M_{23}C_6$. At first, $M_{23}C_6$ core is formed on the grain boundary side and has a specific orientation relationship with the matrix. With the increase of time, the nucleating particles grow preferentially perpendicular to the grain boundary. If the solute supply is sufficient, it eventually leads to the formation of the discontinuous carbide $M_{23}C_6$.

It should be noted that the grain boundaries are broadened and the grains on both sides of the grain boundary are connected by this type of carbide, which will result in a decrease in the bonding force between the grains and increase the sensitivity of the crack initiation therein. When the aging temperature is increased to 830 °C, the number of precipitation phase $M_{23}C_6$ decreases sharply and the size becomes smaller. This is because the nucleation and growth of $M_{23}C_6$ are inhibited by the increase of equilibrium solid solubility of C, Cr and Mo when the aging temperature is higher.

In order to study the effect of the aging time on the precipitation of the precipitated phase, the sample was aged at 800 °C for 48 h, and then the structure and type of the precipitated phase were analyzed by TEM. Fig.7 shows TEM images of intragranular and intergranular precipitates and micro-area electron diffraction patterns. Fig.7a shows that after aging for 48 h, the morphology of the grain boundary and the precipitated phase of the grains change greatly compared with the short-time aging of 2 h, and the

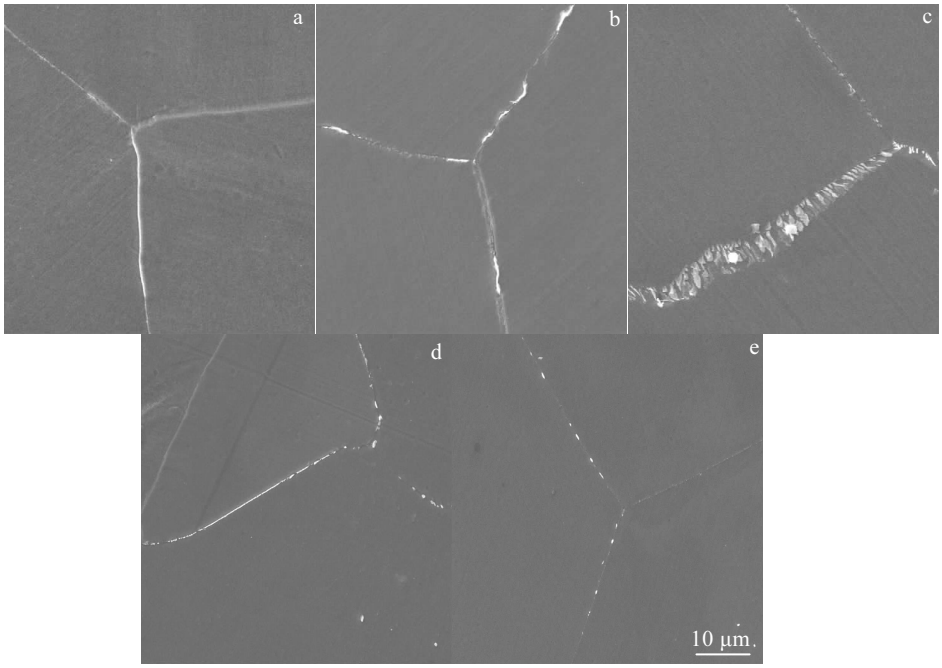

Fig.6 SEM morphologies of precipitated phase at grain boundary after aging at different temperatures for 2 h: (a) 700 °C, (b) 750 °C, (c) 770 °C, (d) 800 °C, and (e) 830 °C

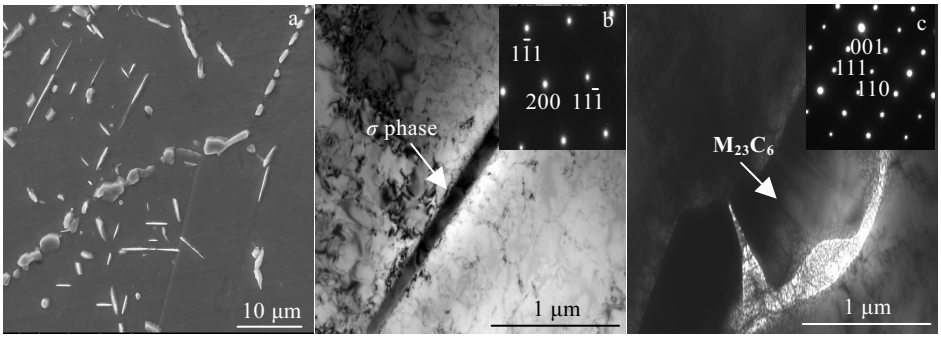

Fig.7 Morphologies and selected area electron diffraction patterns of precipitated phase after aging at 800 °C for 48 h: (a) SEM image, (b) TEM image and SAED pattern of σ phase inside grain, and (c) TEM image and SAED pattern of $M_{23}C_6$ phase from grain boundary

size of the precipitated phase of the grain boundary increases significantly, which is about 3 μm, and the number of precipitated phases increases. The precipitated phases distributes in the grain boundary in a chain-like manner, while there are more needle-like precipitated phases in the grain. It can be seen that the aging time has a significant influence on the precipitated phase. Fig.7b and Fig.7c show that the TEM image and the selected area electron diffraction pattern (SAED) calibration results. It can be seen that the intra-crystalline needle-like precipitated phase is the σ phase of the body-centered cubic structure, and the grain boundary precipitated phase is the face-centered cubic structure of $M_{23}C_6$. This further proves that the nucleation and growth of the σ phase takes a long time, and it is difficult to form in a short term. The precipitation of needle-like or flake-like σ phase in the crystal will seriously reduce the corrosion resistance and the mechanical properties of the alloy [33,34].

From the calculation and experimental results, it can be seen that the G3 alloy has a high content of Cr and Mo. The intermetallic compounds rich in Cr and Mo in the alloy mainly have σ phase and μ phase, and the main carbides are M_6C with Mo and $M_{23}C_6$ with Cr as the main phase. When the alloy is aged at 700~830 °C for 2 h, $M_{23}C_6$ is found in the grain boundary, and no precipitates are observed in the grain. A needle-like σ phase appears in the grain after long-time aging at 800 °C for 48 h, the number and size of $M_{23}C_6$ at grain boundaries increase, and no μ phase and M_6C carbide are found in the aging temperature range of 700~830 °C,

which is consistent with the thermodynamic calculation results. In short, the $M_{23}C_6$ precipitated at the grain boundary and the σ phase precipitated in the grain will make the alloy partially depleted in Cr and Mo, causing structural instability and affecting the service life of the alloy. Therefore, how to reduce or even avoid precipitation in Hastelloy G3 alloy is the key in the production process.

3 Conclusions

1) The main equilibrium precipitates of Hastelloy G3 alloy are the σ phase, μ phase, M_6C and $M_{23}C_6$ carbides. The Cr and Mo contents reduce the initial melting point of the alloy, mainly affecting the precipitation of the σ phase and μ phase and the precipitation temperature; Both Cr and Mo promote the precipitation of the σ phase, Cr inhibits the precipitation of the μ phase, and Mo promotes the precipitation of the μ phase. The Cr and Mo have no significant effect on the precipitation behavior of M_6C and $M_{23}C_6$.

2) The precipitation behavior of M_6C and $M_{23}C_6$ is significantly affected by C element. Excessive C content increases the precipitation tendency of M_6C and $M_{23}C_6$, and the initial precipitation temperature of M_6C and $M_{23}C_6$ also increases significantly.

3) The aging treatment has a great influence on the precipitated phase of the alloy. After a short-time aging at 700~830 °C for 2 h, the precipitated phase appears at the grain boundary and no precipitated phase is found in the grain. After aging at 800 °C for 48 h, the needle-like σ phase is found in the grain, and the number and size of precipitated phase at the grain boundary increase obviously.

References

1 Xiao Guozhang, Gao Xia, Ku Honggang *et al*. *Steel Pipe*[J], 2014, 43(5): 8 (in Chinese)

2 Liu Haiding, Wang Dongzhe, Wei Handong *et al*. *Materials Review* [J], 2013, 27(5): 99 (in Chinese)

3 Chen Changfeng, Jiang Ruijing, Zhang Guoan *et al. Rare Metal Materials and Engineering*[J], 2010, 39(3): 427 (in Chinese)

4 Takeuchi M, Nakajima Y, Hoshino K *et al*. *J Alloy Compd*[J], 2010, 506(1): 194

5 He Daoguang ,Lin Y C, Tang Yi *et al. Materials Science and Engineering A*[J], 2019, 746: 372

6 Li Zhen, Han Jiesheng, Lu Jinun *et al*. *J Alloy Compd*[J], 2015, 619: 754

7 Wang L, Liu F, Cheng J J *et al*. *J Alloy Compd*[J], 2015, 623: 69

8 Jothi Sathiskumar, Merzlikin S V, Croft T N *et al*. *J Alloy Compd*[J], 2016, 664: 664

9 Tian Sugui, Zhang Baoshuai, YHuichen *et al. Materials Science and Engineering A*[J], 2016, 673: 391

10 Khayat Z R, Palmer T A. *Materials Science and Engineering A* [J], 2018, 718: 123

11 Li Helin, Zhang Yaping, Han Lihong. *Steel Pipe*[J], 2007, 36(6): 1 (in Chinese)

12 Anna J, Daniel L, Ulf K. *Corrosion*[C]. Houston: NACE, 2007: 7101

13 Kopliku A, Scoppio L. *Corrosion*[C]. Houston: NACE, 2003: 3128

14 Wang Cheng, Ju Shaohua, Xun Shuling *et al*. *Materials Review*[J], 2009, 23(3): 71 (in Chinese)

15 Masayuki S, Yohei O, Hisashi A *et a1*. *Corrosion* [C]. Houston: NACE, 2011: 11 109

16 Hibner e L, Puckett B C, Patchell J K. *Corrosion*[C]. Houston: NACE, 2004: 4110

17 Tabinor M, Bailey B, Cheldi T *et a1*. *Corrosion*[C]. Houston: NACE, 2006: 6152

18 Li Mingyang, Zhang Qingquan, Wu Huiyun *et a1*. *Research on Metallic Materials*[J], 2014(3): 6 (in Chinese)

19 Bao Yaozong, Dong Han, Su Jie *et a1*. *Special Steel*[J], 2009, 30(5): 1 (in Chinese)

20 Cui Shihua, Li Chunfu, Rong Jinfang *et a1*. *Hot Working Technology*[J], 2009, 38(6): 29 (in Chinese)

21 Qian Jinsen, Chen Changfeng, Li Shengyi *et a1*. *Chinese Journal of Nonferrous Metals*[J], 2012, 22(8): 2214 (in Chinese)

22 Li Dapeng, Lu Minxu, Zhang Lei *et al*. *Journal of Materials Heat Treatment*[J], 2012, 33(S2): 22 (in Chinese)

23 Zhang Xin, Li Hongwei, Zhan Mei. *J Alloy Compd*[J], 2018, 742: 480

24 Wang Hui, Fang Dongmei, Chuang Karl T. *Process Safety and Environment Protection*[J], 2008, 86(4): 296

25 Azevedo Cesar R F. *Engineering Failure Analysis*[J], 2007, 14(6): 978

26 Stefanov P, Stoychev D, Stoycheva M *et al*. *Materials Chemistry and Physics*[J], 2006, 65(2): 212

27 Mudali U Kamachi, Reynders B, Stratmann M. *Corrosion Science*[J], 1999, 41: 179

28 Tang Jiangun, Gong Jianming, Zhang Xianchen, *et al. Engineering Failure Analysis*[J], 2006, 13(7): 1057

29 Tian Wei, Xie Faqin, Zhao Xuehui. *Rare Metal Materials and Engineering*[J], 2012, 41(3): 482 (in Chinese)

30 Li Yuqing, Liu Jinyan. *Grain Boundary Interstitial Phase of Superalloy*[M]. Beijing: Metallurgical Industry Press, 1990: 272 (in Chinese)

31 Su Yuhua. *Master Degree Thesis*[D]. Kunming: Kunming University of Technology, 2008: 10 (in Chinese)

32 Hong H U, Nam S W. *Materials Science and Engineering A*[J], 2002, 332(1-2): 255

33 Lu Jinsheng, Wang Biao, Yao Yingcheng. *Handbook for X-ray Identification of Common Phases in Steel and Alloys*[M]. Beijing: Beijing General Institute of Iron and Steel Research, 1990: 63 (in Chinese)

34 Wang Baoshun, Luo Kunjie, Zhang Maicang *et al. World Iron & Steel*[J], 2009, 9(5): 42 (in Chinese)

镍基耐蚀 Hastelloy G3 合金的组织特征及热力学计算

赵振铎[1]，李　莎[1]，范光伟[1]，李建春[2]

(1. 太原钢铁（集团）有限公司 先进不锈钢材料国家重点实验室，山西 太原 030003)

(2. 山西太钢不锈钢股份有限公司 技术中心，山西 太原 030003)

摘　要：利用 Thermo-Calc 软件对镍基耐蚀 Hastelloy G3 合金进行了热力学计算，系统研究了成分对平衡相析出的影响规律，并通过 SEM 和 TEM 对合金时效处理后的析出相进行了观察。结果表明，合金析出的平衡相主要为 σ 相、μ 相、M_6C 和 $M_{23}C_6$；Cr 和 Mo 的含量主要影响 σ 相和 μ 相的析出和初始析出温度；而 C 元素含量显著影响碳化物 M_6C 和 $M_{23}C_6$ 的析出行为；通过实验进一步研究了时效过程中析出相的析出规律。

关键词：Hastelloy G3合金；热力学计算；析出相；时效处理

作者简介：赵振铎，男，1980 年生，博士，教授级高级工程师，太原钢铁（集团）有限公司先进不锈钢材料国家重点实验室，山西 太原 030003，电话：0351-2130309，E-mail: zhaozd@tisco.com.cn